Investigation on small-scale low pressure LNG production process

Published Version:
Ancona, M., Bianchi, M., Branchini, L., De Pascale, A., Melino, F., Mormile, M., et al. (2018). Investigation on small-scale low pressure LNG production process. APPLIED ENERGY, 227, 672-685 [10.1016/j.apenergy.2017.08.084].

Availability:
This version is available at: https://hdl.handle.net/11585/624594 since: 2020-02-27

Published:
DOI: http://doi.org/10.1016/j.apenergy.2017.08.084

This is the final peer-reviewed accepted manuscript of:

Maria Alessandra Ancona, Michele Bianchi, Lisa Branchini, Andrea De Pascale, Francesco Melino, Mario Mormile, Marco Palella, Luigi Benedetto Scarponi,

Investigation on small-scale low pressure LNG production process,

Applied Energy, Volume 227, 2018, p. 672-685

The final published version is available online at:
https://doi.org/10.1016/j.apenergy.2017.08.084

INVESTIGATION ON SMALL-SCALE LOW PRESSURE LNG PRODUCTION PROCESS

M. A. Ancona[a], M. Bianchi[a], L. Branchini[a], A. De Pascale[a], F. Melino[a], M. Mormile[b], M. Palella[b], L.B. Scarponi[c,]*

[a] DIN– Alma Mater Studiorum, University of Bologna, viale del Risorgimento 2, 40136, Bologna ITALY
[b] Graf S.p.a. – Via Galileo Galilei 36, 41015 Nonantola (MO) ITALY
[c] CIRI-EA – Alma Mater Studiorum, via Angherà, 22, 47900 Rimini, ITALY

*****corresponding author: e-mail: luigi.scarponi2@unibo.it, phone: +39-051-2093320

ABSTRACT

With the increase of global energy demand, the natural gas will play a key role both for energy production and for transports. Typically, natural gas is extracted and liquefied in large-scale plants to be later transported by ship or, when it is possible, by pipeline. In this study, a *plug & play* solution for natural gas liquefaction to be directly installed at the vehicle's filling stations, in order to avoid the transport costs of liquefied natural gas, is analyzed. The system analyzed in the paper consists in a single stage expansion process and the aim of the study is to improve the small-scale liquefaction process efficiency through the use of a cryogenic expander in replacement of a more common Joule-Thomson valve. A thermodynamic study has been carried out to optimize the process parameters with the aim of minimizing the energy consumption. This optimization study, starting from a reference case, allowed to identify an optimal case, which leads to a total energy saving of about 12 % compared to the reference case. Furthermore, considerations relating to the cryogenic expander, which is a key component of the system, have been done. This device guarantees a higher thermodynamic efficiency than Joule-Thomson valve and it allows to integrate the produced shaft power into the process. This study represents a preliminary thermodynamic and parametric investigation on a low pressure LNG production process. The results of this study are the basis for the realization of a prototype which is actually under construction. Thus, further investigations by Authors will determinate the techno-economic feasibility of the optimized system also considering future experimental investigations.

NOMENCLATURE

A	pressure losses coefficient [-]
a	conversion coefficient [m/ft]
c_p	specific heat at constant pressure [kJ/kg]
c_v	specific heat at constant volume [kJ/kg]
D	characteristic dimension [m]
e	total specific electric energy consumption [kJ/kg]
g	gravitational acceleration [m/s^2]
h	enthalpy [kJ/kg]
H_{ad}	adiabatic head [m]
k	heat capacity ratio [-]
$\dot{m}$	mass flow rate [kg/s]
N	rotational speed [rpm]
P	power [kW]
p	pressure [bar]
T	temperature [°C]
V	volume flow rate [m^3/s]
x	quality [-]

Greek Symbols

β	pressure ratio [-]
Δ	difference [-]
ε	heat exchangers effectiveness [-]
η	efficiency [-]

Subscripts and Superscripts

1,…,15	process sections of main interest
C	compressor

chiller compression chiller
exp expander
is isentropic
p polytropic
s specific
tot total

Acronyms

EER Energy Efficiency Ratio
HE Heat Exchanger
LNG Liquefied Natural Gas
MTPA Million Tons Per Annum
NG Natural Gas
TV Throttle Valve

1 INTRODUCTION

The growth of global population and developing countries led to an increasing global energetic demand [1]. In the next decades, the renewable energy sources will cover only a small portion of this request, which will continue to be satisfied principally by fossil fuels [1]. With increasingly stringent legislation on environmental pollution, the Natural Gas (NG) will play a fundamental role [2]. Indeed, it is the most "eco-friendly" energy source among others fossil fuels [3-9]. In this scenario, where the NG will play a fundamental role, both for energy production and for transports, the Liquefied Natural Gas (LNG) will be a promising solution.
The liquefaction process significantly increases the NG density; indeed the LNG density is about 600 times higher than that of NG [10], in this way the storage volumes are reduced, thereby facilitating the transport. With reference to ambient pressure, the boiling point of NG is about -162°C [11], then liquefaction process requires a cooling of the NG using various cryogenic processes. The main are:

- cascade cycle: it is a succession of several compression cycles. The fluids used in the cascade process have a decreasing triple point temperature. This prevents freezing with cryogenic temperatures. This kind of process is relatively simple and reliable [12-17];
- mixed refrigerant cycle: it consists of a single stage cycle; the refrigerant is typically a mixture of methane, ethane, i-butane, n-butane and nitrogen [18-24];
- expander cycle: a compressor followed by an expander, which work with a single component gas stream, compose the refrigeration cycle [24-30].

The processes described above are mostly used in large-scale plants, which have a capacity greater than 5 Million Tons Per Annum (MTPA) [31]. Typically, the LNG is produced by large-scale liquefaction plants and then transported by the means of LNG carriers. In **Figure 1,** the percentage of average capital costs for each step in the LNG value chain are shown [32].

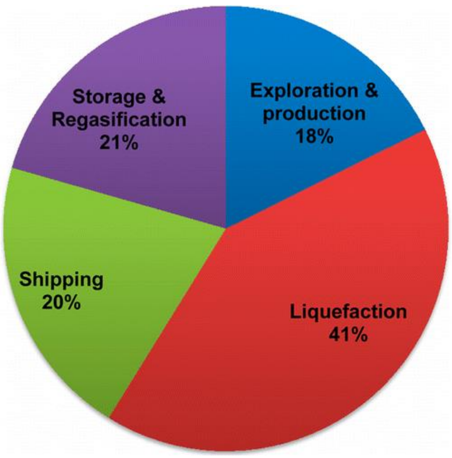

Figure 1 - Cost breakdown of the LNG value chain [32].

With technological improvements in recent years, small-scale plants become very interesting. A liquefaction plant is considered small-scale if it produces less than 1 MTPA of LNG [33]. This kind of plants are used for reasons that vary from limited space available for the installation to areas with low energy demand [34]. In small-scale NG liquefaction plants, single mixed-refrigerant (SMR) [35] and N_2 expander cycle [36] are the most widespread liquefaction processes. The SMR process efficiency strongly depends on the optimization of mixed refrigerant composition and on the ambient conditions [35], the power consumption of this process is usually lower than the N_2 expander cycle. On the other hand, the efficiency of the latter is almost independent of feed gas condition. Moreover, nitrogen is a nonreactive refrigerant, then the safety is greater [37]. Yuan et al. have studied a small-scale NG liquefaction process adopting single nitrogen expansion with the aim of minimizing the unit energy consumption. They demonstrate that the system is compact, reliable and it shows a good adaptability to the feed gas condition [38]. He and Ju presented a novel NG liquefaction process that allows to liquefy, without energy consumption, part of NG employing the pressure exergy of the pipeline. The system efficiency depends on the pipeline pressure, if it is too low the process may not work [39]. Kim et al. proposed a LNG supply chain using liquid nitrogen for the NG liquefaction. This system allows to avoid related costs to regasification by an efficiently use of cold energy of both LNG and liquefied nitrogen. A key parameter of this process is the distance between the LNG and liquefied nitrogen production sites [37]. Jokinen et al. presented a mathematical model to optimize a small-scale LNG supply chain [40]. Differently from the above-mentioned works, the study presented in this paper is an optimization of small-scale LNG production plant, which is mainly focused on the device and parameters concerning the NG side. In particular, this solution is designed to be directly installed at the vehicle's filling stations, in this way the costs relative to the transport of LNG are avoided. With reference to **Figure 1**, it must be highlighted that the transport costs are not negligible, then their avoidance implies a considerable economic saving. This paper is the development of Authors' preliminary works [41,42], thus the results earlier obtained have been considered for the analysis carried out in this study. The peculiarity of the system described in this paper is the presence of a two-phase cryogenic expander, which replaces the more common Joule-Thomson valve in the lamination process. This configuration, how it will be demonstrated in the following paragraphs, leads to a lower energy consumption of the process. LNG cryogenic two-phase expander is a well-established technology in large-scale plants [43]; nevertheless, to the Authors' knowledge, this solution is a novelty for a small-scale plant. In this paper a thermodynamic analysis has been carried out in order to find an optimal configuration of the system in terms of energy consumption. The Authors will assess the economic aspects in future studies because of the novelty of the process, referring to the small-scale LNG production, but mostly to the lack of information about the two-phase cryogenic expander, both in literature and in the market.

The paper is structured as follows: section 2 presents the process description; section 3 illustrates the hypothesis made and the studied parameters; section 4 describes the parametric analysis results, starting from a reference case, moreover it is present a follow-up study about the cryogenic expander; finally, section 6 highlights concluding remarks.

2 PROCESS DESCRIPTION

The layout of the liquefaction process analyzed in this paper is shown in **Figure 2**. The natural gas, coming from the grid (section 1), is mixed with the gaseous stream extracted from the flash tank (12-15). The resulted stream (2) is compressed by a compression train (2-6). The compression is inter-cooled (3-4) and after-cooled (5-6) by air cooled heat exchangers. After the compression, the NG stream is firstly pre-cooled by heat exchanger HE-1 (6-7), by means of the stream coming from the flash tank as cold source. Afterwards, NG is cooled by a compression chiller (8) HE-2. Finally, the stream passes through HE-3, reaching the physical state (9). Thus, the NG stream crosses a two-phase cryogenic expander where its pressure and its enthalpy decrease (10). It should be highlighted that at the inlet of the expander (9) the NG stream is in the physical conditions of supercritical state, while at the outlet (10) it is in two-phase conditions. Passed the expander, the stream reaches a flash tank where the liquefied natural gas (11) is extracted to be stored, while the vapor fraction is used in the heat exchangers to cool down the main NG stream, with which it is finally mixed, as described above. It should be highlighted that valve TV, between sections (12) and (13), has been introduced for the parametric analysis that will be discussed in the following paragraphs. The valve is only required where the storage pressure (p_{10}) and the NG feeding grid pressure (p_1) are different (unless the pressure losses).

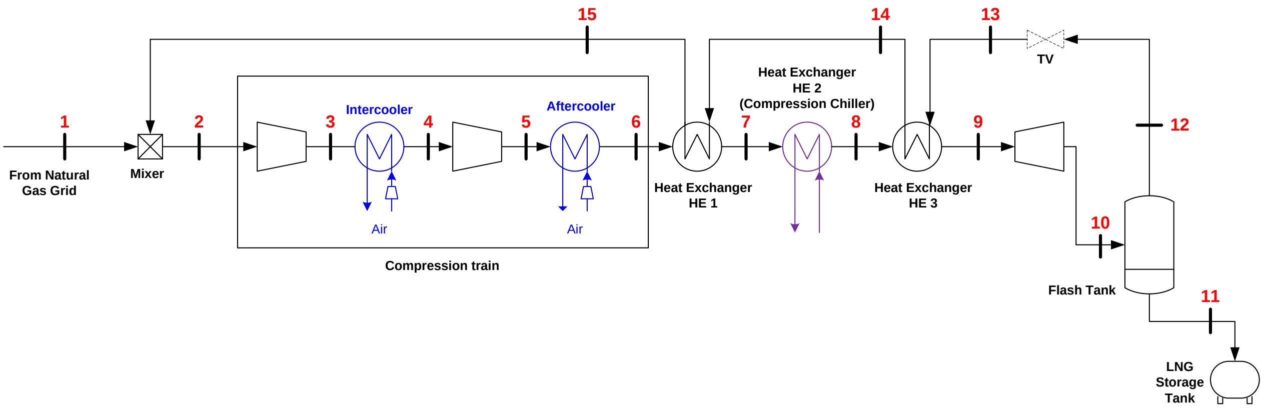

Figure 2 - Layout of natural gas liquefaction process.

3 METHODOLOGY

For the thermodynamic analysis of the liquefaction process, an in-house developed software has been realized. This software allows to simulate the entire process by calculating all the parameters useful to its characterization. The computation is based on iterative resolution of mass and energy balances calculated on each component of the system by the use of a trial-and-error procedure.

In this software, a database of fluids [44] has been implemented. This allows to determinate the physical state of the fluid in each section of the process. The simulation is a steady-state analysis.

The inputs required by the software for the computation are:

- characteristic of NG stream (pressure, temperature…) coming from the grid (section 1);
- compression ratios of the compressors (that determines the maximum pressure of the process);
- polytropic (η_p) efficiency of compressors;
- isentropic (η_{is}) efficiency of the expander;
- the inter-cooling and after-cooling temperatures (T_4 and T_6);
- the effectiveness (ε) of heat exchangers HE-1 and HE-3;
- the outlet temperature of compression chiller (T_8);
- the EER – Energy Efficiency Ratio of the compression chiller;
- the refrigeration fluid of the compression chiller;
- the pressure drops for each heat exchanger (expressed as percentage of the inlet pressure);
- pressure of the storage tank (p_{10});
- the LNG mass flow rate at the outlet of the flash tank ($\dot{m}_{LNG}$, section 11);

With these inputs the following parameters can be determined:

- temperature, pressure, enthalpy, quality and mass flow rate in each section;
- heat transfers;
- specific electric energy consumption of the compressors (e_C);
- specific electric energy consumption of the compression chiller ($e_{chiller}$);
- specific electric energy production of the expander (e_{exp});
- total specific electric energy consumption of the system (e_{tot}).

In detail

$$e_{tot} = e_C + e_{chiller} - e_{exp} \tag{1}$$

where:

- the specific electric energy consumption, introduced in [28] is expressed in [kJ/kg$_{LNG}$] and defined as:

$$e = \frac{P_i}{\dot{m}_{LNG}} \tag{2}$$

where:

- P_i [kW] is the generic electric power required/produced by the i-component;
- $\dot{m}_{LNG}$ [kg/s] is the mass flow rate of LNG at the outlet of the flash tank (section 11). In the parametric analysis, $\dot{m}_{LNG}$ is set to 1 kg/s to have a unit value. Moreover, this value assures to come under the category of small-scale plants (LNG production lower than 1 MTPA, which corresponds to a value close to 30 kg/s) [33].

3.1 Hypothesis

For the analysis presented in this paper several assumptions have been made. All the hypothesis are summarized in **Table 1**. The NG composition is assumed to be 100% CH_4. Therefore, percentages of different substances such as CO_2, N_2 or other hydrocarbons, have not been taken into account. Anyway, the resulting error in this assumption is negligible because Authors in a preliminary study [41] proved that the presence of these components does not significantly change the results. The same pressure drops are considered for each heat exchanger. The compression process is thought to be divided in two sections. This allows to reduce the energy consumption by using inter-cooling and after-cooling HE. To distribute the total compression ratio between the two compressors, an optimization criterion to minimize the specific compression work has been developed in [41]. This criterion takes into account the pressure drops through the heat exchangers. Thus for the first compressor of the compression train the design pressure ratio can be estimated as:

$$\beta_1 = \left(\frac{T_5}{T_3}\right)^{\frac{\eta_P}{2}\cdot\frac{k}{k-1}} \cdot \frac{1}{A} \cdot \sqrt{\beta_{\mathrm{tot}}} \qquad (3)$$

while for the second compressor the design pressure ratio can be estimated as:

$$\beta_2 = {}^{\beta_{tot}}\!/_{\beta_1} \qquad (4)$$

where:

- β_{tot} is the total compression ratio (p_6/p_2) [-];
- T is the temperature expressed in Kelvin [K];
- η_p is the polytropic efficiency of the compressors [-];
- k is the heat capacity ratio (c_p/c_v) for CH_4;
- A is a coefficient introduced to consider the pressure drops through the inter-cooler and the after-cooler. This coefficient is defined as:

$$A = {}^{p_4}\!/_{p_3} = {}^{p_6}\!/_{p_5} \qquad (5)$$

A detailed analytical demonstration of the above-written equation is presented in [41].

Table 1 - Input of the reference case of liquefaction process.

Input variable	symbol	unit of measurement	value
NG composition	-	[-]	100% CH_4
Feed temperature of NG stream (section 1)	T_1	[°C]	20
Feed pressure of NG stream (section 1)	p_1	[bar]	3.0
Polytropic efficiency of the compressors	η_p	[-]	0.565
Maximum pressure of the cycle (section 6)	p_6	[bar]	200
Pressure drops in heat exchangers	Δp	[%]	2
Inter-cooling and after-cooling exit temperature	$T_4 = T_6$	[°C]	30
Heat exchange efficiency of HE-1 and HE-3	ε	[%]	70
Outlet temperature of the chiller (section 8)	T_8	[°C]	-50
Energy Efficiency Ratio of the chiller	EER	[-]	1.1
Isentropic efficiency of the expander	η_{is}	[-]	0.7
Mass flow rate of LNG (section 11)	$\dot{m}_{LNG}$	[kg/s]	1
Storage pressure (section 10)	p_{10}	[bar]	3.1
Electro-mechanical efficiency of the compressors	η_{em}	[-]	0.95

3.2 Parametric analysis

In this paper, starting from the reference case of liquefaction process, described in the previous paragraph, a parametric analysis has been carried out. This analysis has the aim to find out the configuration of the system that leads to a minimum energy consumption. In particular, the influence of maximum cycle pressure (p_6), storage pressure (p_{10}), compression chiller outlet temperature (T_8) and isentropic efficiency of the expander (η_{is}) has been analyzed. Considering the ease of the proposed system, these are the main parameters that can be evaluated, through a complete thermodynamic analysis, to find an optimal configuration of the process. In details:

- maximum pressure of the process (p_6) varies from 200 to 300 bar[1];
- storage pressure (p_{10}) varies from 3 to 15 bar[1];
- outlet temperature of the compression chiller (T_8) varies from -15 to -50 °C[1];
- isentropic efficiency of the expander (η_{is}) varies from 0 % (the expander is replaced with a Joule-Thomson valve) to 100 % (ideal case).

The trends of the influence of the studied parameters on the system performances are predictable. Since, a parametric analysis is suitable to find an optimal solution.
In the analysis, these parameters have been varied one by one, while the others remain unchanged, in order to see the consequences related to the changes of each parameter.

4 RESULTS

In the following paragraphs, the results of the carried out parametric analysis are shown. Starting from the reference case, the thermodynamic state in each section of the process, the energy consumption and the heat exchanges are calculated. Afterwards, the results related to the optimal case, identified through the parametric analysis, are described.

4.1 Reference case results

The reference case layout is shown in **Figure 2**, while the relative thermodynamic diagram *Log p-h* is represented in **Figure 3**. In the reference case, the TV valve between section (12) and (13) has been ignored. This because the storage pressure (p_{10}) is almost the same of the feed pressure of NG stream (p_1). To be more precise, the storage pressure is 3.1 bar, a value slightly higher than the pressure in section 1, evidently due to the pressure losses between the storage tank and the mixer. This allows the vapor fraction, extracted by the flash tank, to overcome the pressure drops in the heat exchangers HE-3 and HE-1, reaching the same pressure of the feed NG stream. The results of the simulation are reported in **Table 2**, where the values of pressure, temperature, mass flow rate and quality, in each section, are indicated. Since a steady-state analysis has been considered, it can be noticed that the value of the mass flow rate in the inlet section (1) and in the outlet one (11) are the same. It is recalled that the value of $\dot{m}_{LNG}$ is set to 1 kg/s, as specified in the hypothesis of the previous paragraph. **Table 3** shows the energy results in terms of specific electric energy consumption and heat transfer.

Table 2 - Thermodynamic state in each section for the reference case.

Section	**Pressure** [bar]	**Temperature** [°C]	**Mass Flow Rate** [kg/s]	**Quality** [-]
1	3.0	20	1.000	-
2	3.0	9	1.927	-
3	26.0	284	1.927	-
4	25.5	30	1.927	-
5	203.7	304	1.927	-
6	199.7	30	1.927	-
7	195.8	7	1.927	-
8	192.0	-50	1.927	-
9	188.2	-67	1.927	-
10	3.1	-145	1.927	0.481
11	3.1	-145	1.000	0
12	3.1	-145	0.927	1
13	3.1	-145	0.927	1
14	3.1	-76	0.927	-
15	3.0	-2	0.927	-

[1] The proposed ranges are in line with the components available on the market.

Table 3 - Energy results for the reference case.

Components	Electric Energy Consumption [kJ/kg$_{LNG}$]	Electric Energy Production [kJ/kg$_{LNG}$]	Thermal Exchange [kJ/kg$_{LNG}$]
Compressors	2775	-	-
Compression chiller	407	-	-
Expander	-	138	-
Inter-cooler	-	-	1333
After-cooler	-	-	1685
Heat exchanger HE-1	-	-	154
Heat exchanger HE-3	-	-	136
TOTAL	**3182**	**138**	**3308**

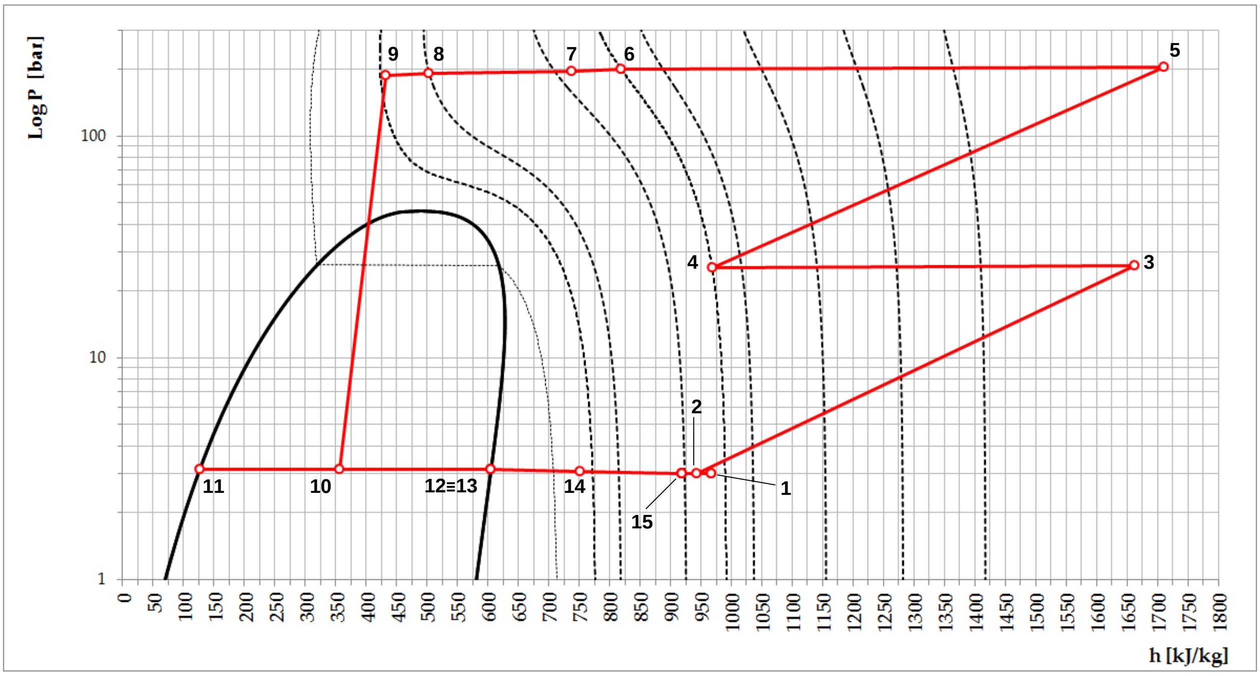

Figure 3 - Thermodynamic diagram Log p-h of natural gas liquefaction process for the reference case.

The vapor fraction sharply depends by the value of the quality at the outlet of the expander, (section 10). Since the produced LNG mass flow rate is set, a lower value of quality leads to a lower vapor mass flow rate. This means that the compressors and the heat exchangers work with a lower mass flow rate, then the total electric energy consumption decreases. The proposed process involves the use of a two-phase cryogenic expander, instead of the more common layouts that use a Joule-Thomson valve. The use of an expander has several key features:

- the expansion implies an enthalpy reduction that means a lower value of the quality at the outlet section of the expander;
- the thermodynamic efficiency of an expander is higher than the more common Joule-Thomson valve [45];
- the produced shaft power is integrated into the process; thus it minimizes the external electric energy consumption of the cycle;

The position of heat exchangers in the plant ensures that the inlet temperature of the compression train (section 2) keeps higher than the minimum permitted temperature for the integrity of compressors. Based on manufacturer’s information, this minimum value is close to -10 °C.

4.2 Parametric analysis results

In this paragraph, the results of the parametric analysis are shown, with reference to the layout represented in **Figure 2**. The throttle valve, introduced between sections (12) and (13), allows to adjust the pressure set in the flash tank, to the one of the feeding grid. Starting from the study of the influence of the maximum cycle pressure (6) and of the compression chiller outlet temperature (8), with storage pressure set to 3.1 bar (10), in **Errore. L'origine riferimento non è stata trovata.** is shown the total specific electric energy consumption of the system. In **Figure A1** of Appendix A are respectively shown: a) specific electric energy consumption of the compressors, b) specific electric energy consumption of the chiller, c) specific electric energy produced by the expander, d) total specific electric energy consumption of the system. The specific electric consumption/production are referred to the mass of LNG produced. It can be seen that, the higher is the maximum pressure, the higher is the total electric consumption (**Figure 4**). Anyway, the energy consumption/production in the case with p_6 = 300 bar it is only slightly higher than that in the case with p_6 = 200 bar. Therefore, the maximum pressure of the cycle does not significantly influence the system performances in terms of energy consumption. Contrarily, the outlet temperature of the compression chiller (T_8) has a key role. Indeed, especially for the electric energy consumption of the compressors, from **Figure A1a** it can be noticed that the lower is the T_8, the lower is the electric energy consumption. For the reference case, considering a value of T_8 = -15 °C, the electric energy consumption of the compressors is slightly less than 3800 kW. On the other hand, with T_8 = -50 °C, a decrease up to less than 2800 kW is observed. This behavior is a consequence of the quality reduction at the outlet of the expander, caused by the decrease of the outlet temperature of the compression chiller showed in **Figure 5** that will be hereunder examined. **Figure A1b** shows the electric consumption of the chiller. Obviously, the lower is the outlet temperature, the higher is the chiller consumption. From **Figure A1c**, it can be seen that the energy produced by the expander decreases with the reduction of the outlet temperature of the chiller. It should be emphasized that the energy consumption/production of the chiller and of the expander, if compared to the one of the compressor (**Figure A1a**), are of an order of magnitude lower.

The**Errore. L'origine riferimento non è stata trovata. Figure 5** shows the trend of the quality at the outlet of the expander (10). As it can be seen the value of the quality decreases with the increase of maximum pressure and with the decrease of the outlet temperature of the chiller. A lower quality leads to a lower mass flow rate to be elaborated by compressors. Then, this would mean an energy saving. Conversely, the total energy consumption, necessary to reach higher pressure, and consequently to decrease the value of the quality, is greater than the benefits caused by a quality reduction. Indeed, as shown in **Errore. L'origine riferimento non è stata trovata.**, the minimum of total energy consumption is achieved with a maximum pressure of 200 bar.

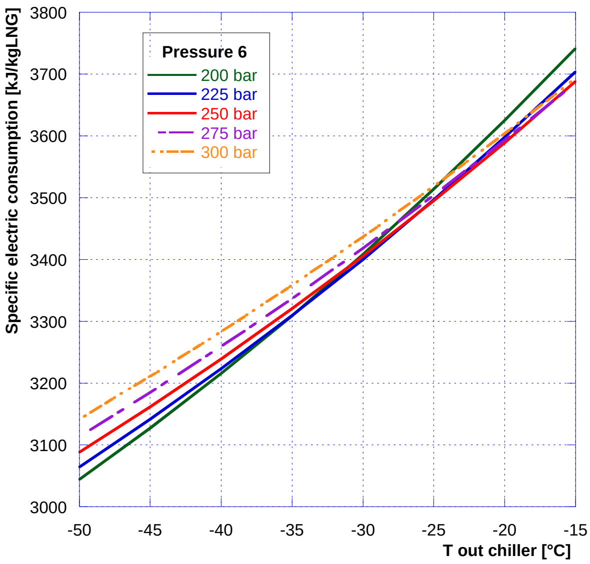

Figure 4 - Total specific electric energy consumption of the system as function of the outlet temperature of the chiller (T_8) for several values of maximum pressure $p_{6,}$ with a set value of storage pressure p_{10} = 3.1 bar.

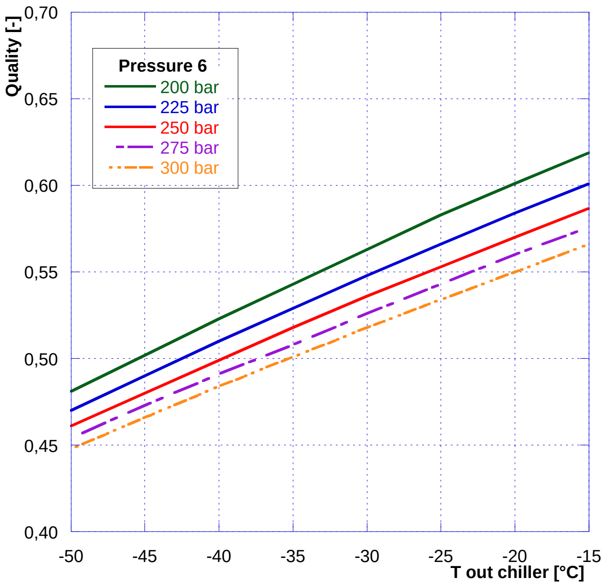

Figure 5 - Quality at the outlet of the expander (section 10) as function of the outlet temperature of the chiller (T_8) for several values of maximum pressure $p_{6,}$ with a set value of storage pressure $p_{10} = 3.1$ bar.

The sensitivity analysis on storage pressure influence shows that this parameter strongly affects the system performances. In this analysis the outlet temperature of compression chiller (T_8) is set to the value of -50 °C. **Figure 6** and **Figure 7** respectively show the trend of the total specific electric energy consumption of the system and of the quality at the outlet of the expander (section 10), as function of the cycle maximum pressure (p_6), for several values of the storage pressure (p_{10}). Relatively to **Figure 7**, it can be noticed that, the higher is the storage pressure (p_{10}), the lower is the quality at the outlet of the expander. This behavior can be explained analyzing the Log p-h diagram (**Figure 3**). The positive slope of the liquid saturation curve means that, considering two points with the same enthalpy, but at different pressures, inside the two-phase field, the one at higher pressure has a lower quality. The **Figure 6 A2,** in Appendix A, shows that an increase of the storage pressure leads to a lower energy consumption/production of the components. In detail, as it can be seen from **Figure 6**, the higher is the storage pressure, the lower is the total energy consumption of the system. Moreover, as stated above, it can be emphasized that the total energy consumption is relatively unaffected by maximum pressure of the cycle. Since the LNG mass flow rate is fixed to the value of 1 kg/s, the decrease of the quality caused by the increase of the storage pressure, leads to a lower vapor mass flow rate extracted by the flash tank. Therefore, the compressors, working with a lower mass flow rate, consume less energy. The trend of the mass flow rate through the expander is shown in **Figure 8**. As mentioned above, an increase of the cycle maximum pressure and of the storage pressure leads to lower value of the mass flow rate through the compressor and thus also through the expander. This implies a lower energy production by the expander. On the other hand, considering that the compression train is the device which weight more in terms of system energy consumption, it is advantageous to have a lower mass flow rate rather than favour the expander energy production.

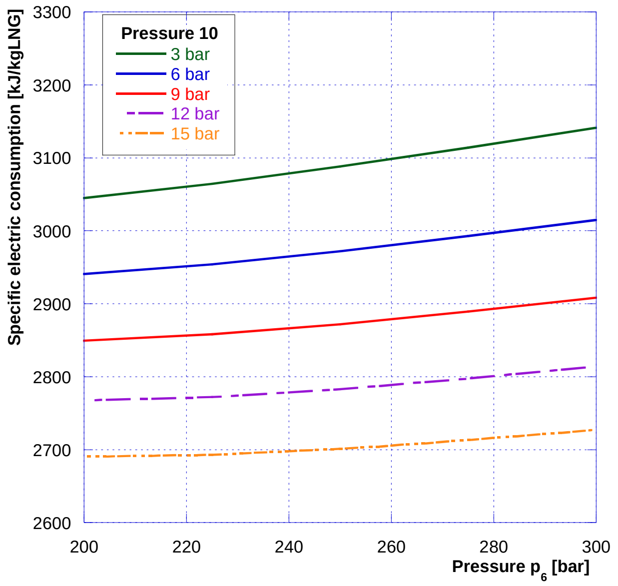

Figure 6 - Total specific electric energy consumption of the system as function of maximum pressure p_6, for several values of storage pressure p_{10} and a set value of T_8 = -50 °C.

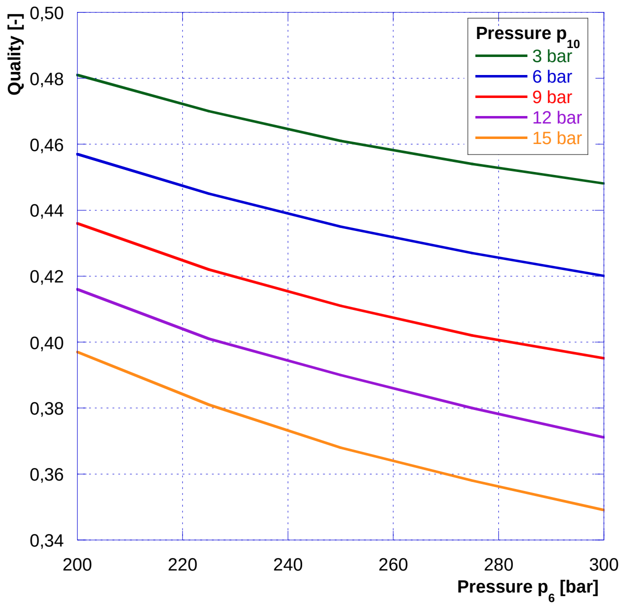

Figure 7 - Quality at the outlet of the expander (section 10) as function of maximum pressure p_6 for several values of storage pressure p_{10} and a set value of T_8 = -50 °C.

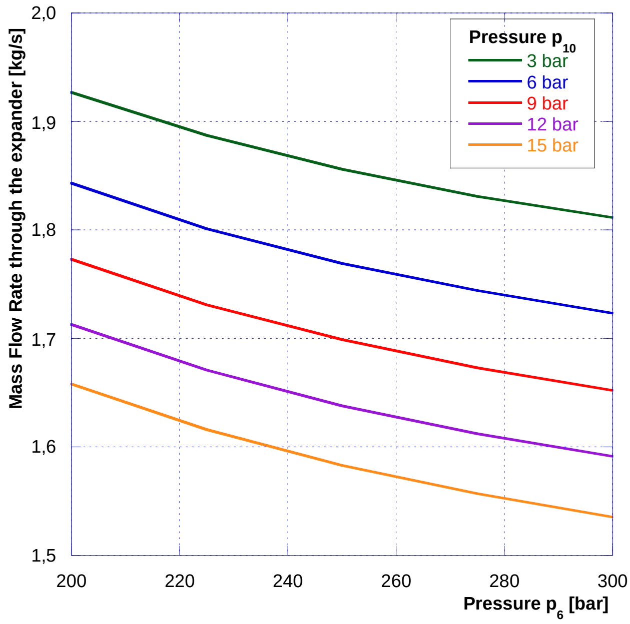

Figure 8 - Mass flow rate through the expander as function of maximum pressure p_6 for several values of storage pressure p_{10} and a set value of T_8 = -50 °C.

The trend of the total specific electric energy consumption of the system and of the quality at the outlet of the expander, as function of the outlet temperature of the chiller (T_8), for several values of the storage pressure (p_{10}) are respectively shown in **Figure 9** and **Figure 10**. (In **Figure A3** of Appendix A are shown the trends of the specific electric energy consumption/production of the various devices of the system). In this case too, it can be noticed that the lower is the T_8 and the higher is p_6, the lower will be the total electric energy consumption. The same reasoning applies to the trend of the quality (**Figure 10**).

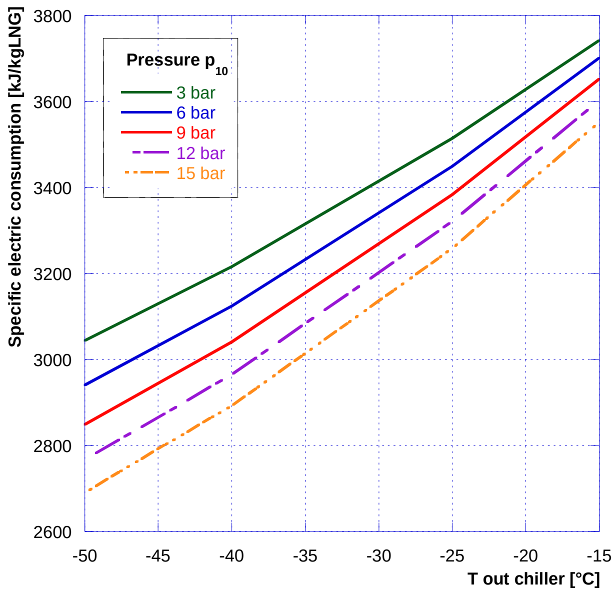

Figure 9 - Total specific electric energy consumption of the system as function of outlet temperature of the chiller T_8, for several values of storage pressure p_{10} and a set value of maximum pressure p_6 = 200 bar.

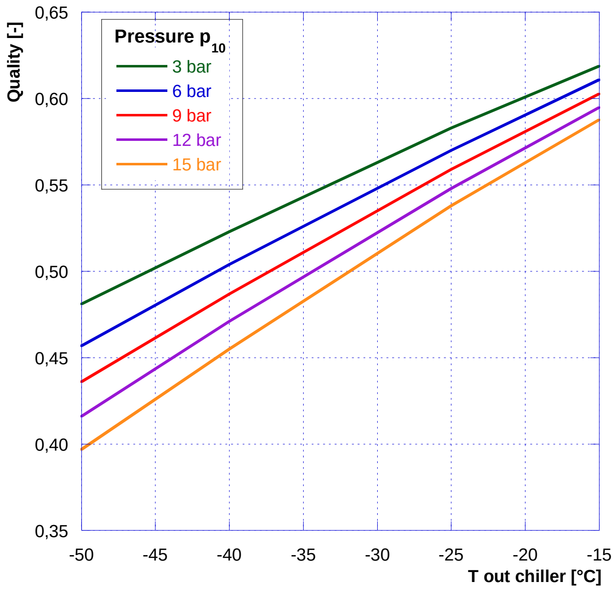

Figure 10 - Quality at the outlet of the expander (section 10) as function of outlet temperature of the chiller T_8, for several values of storage pressure p_{10} and a set value of maximum pressure p_6 = 200 bar.

As a result of the carried out parametric analysis, it has been identified an optimal system configuration, in terms of energy consumption. The optimal solution has been identified through the analysis of **Figure 11** which represents the trend of the total specific electric energy consumption as function of the maximum pressure of the cycle (p_6) and the storage pressure (p_{10}), for several values of the chiller outlet temperature (T_8). It can be noticed that this solution is achieved by working with a maximum cycle pressure of 200 bar, a storage pressure of 15 bar and with a compression chiller outlet temperature of -50 °C. The results related to the optimum case are summarized in

Table 4 and

Table 5.

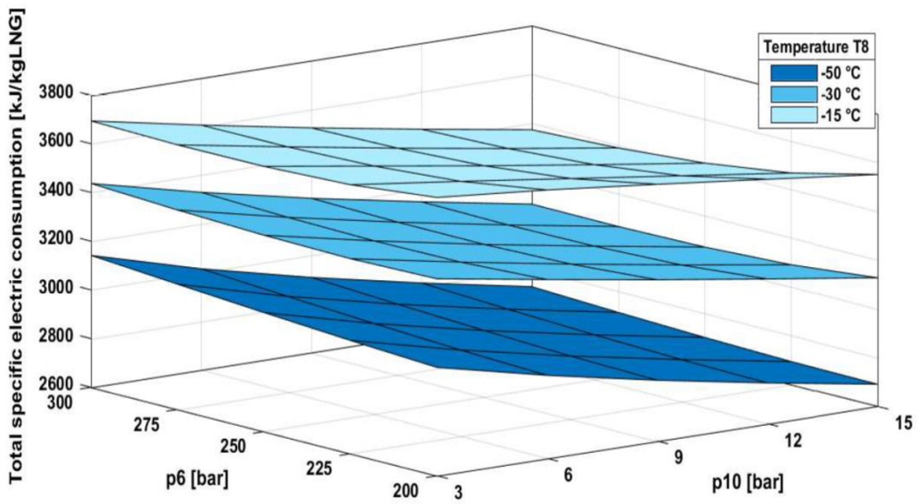

Figure 11 - Total specific electric energy consumption of the system as function of maximum pressure of the cycle p_6, storage pressure p_{10}, for several values of outlet temperature of the chiller T_8.

Table 4 - Thermodynamic state in each section for the optimum case.

Section	**Pressure** [bar]	**Temperature** [°C]	**Mass Flow Rate** [kg/s]	**Quality** [-]
1	3.0	20	1.000	-
2	3.0	12	1.658	-
3	26.0	288	1.658	-
4	25.5	30	1.658	-
5	203.7	305	1.658	-
6	199.7	30	1.658	-
7	195.8	11	1.658	-
8	192.0	-50	1.658	-
9	188.2	-63	1.658	-
10	15.0	-115	1.658	0.397
11	15.0	-115	1.000	0
12	15.0	-115	0.658	1
13	3.1	-136	0.658	-
14	3.1	-76	0.658	-
15	3.0	-1	0.658	-

Table 5 - Energy results for the optimum case.

Components	**Electric Energy Consumption** [kJ/kg$_{LNG}$]	**Electric Energy Production** [kJ/kg$_{LNG}$]	**Thermal Exchange** [kJ/kg$_{LNG}$]
Compressors	2396	-	-
Compression chiller	375	-	-
Expander	-	81	-
Inter-cooler	-	-	1164
After-cooler	-	-	1450
Heat exchanger HE-1	-	-	106
Heat exchanger HE-3	-	-	86
TOTAL	**2771**	**81**	**2806**

Comparing the results for the reference case and the optimum case, it can be noticed that the most influenced parameter is the electric consumption of the compressors. Contrarily, the electric energy consumption of the compression chiller and the energy produced by the expander slightly decrease. Comparing

Table 4 and **Table 5**, it can be noticed that also the heat exchanges are lower in the optimum case. This is due to the smaller mass flow rate. In **Table 6** the comparison of the different case results is shown.

Table 6 – Comparison between reference and optimum cases.

	Reference case [kJ/kg$_{LNG}$]	**Optimum case** [kJ/kg$_{LNG}$]	**Percentage variation** [%]
Compressor electric consumption	2775	2396	-14
Chiller electric consumption	407	375	-8
Expander electric production	138	81	-42
Total electric consumption	**3044**	**2690**	**-12**

The total electric consumption of the optimum case is reduced down to 12 % compared to the reference case. This is principally due to the decrease of the mass flow rate elaborated by the compressors, which decreases his value from 1.927 kg/s, of the reference case, to 1.658 kg/s, of the optimum case. In **Figure 12** the thermodynamic diagram *Log p-h* for the optimum case is shown and compared with the reference case.

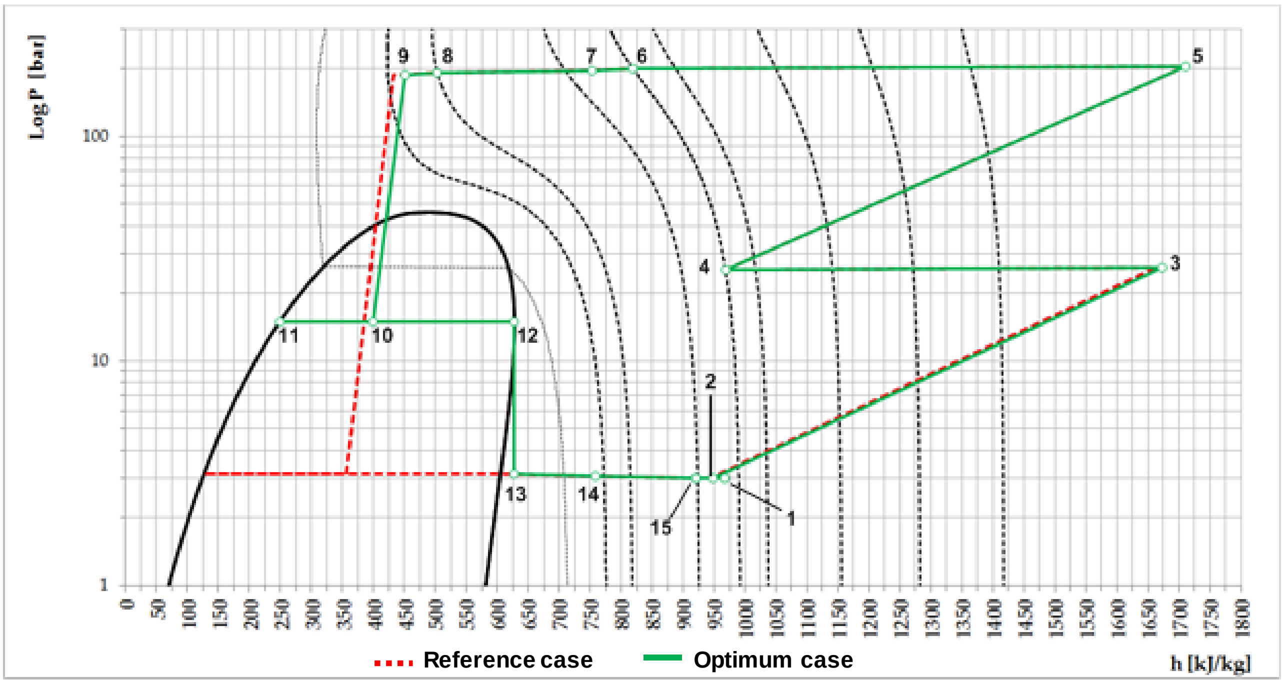

Figure 12 - Thermodynamic diagram of the process obtained for the optimum case (in green) and comparison with the reference case cycle (dotted red line).

With reference to **Figure 12** it can be noticed that the process cycles related to the reference and optimum case are similar. The main differences start from point 9; in the reference case is at temperature of -67 °C, lower compared with the optimum case in which is -63 °C. The point 10, in the optimum case, has a pressure value of 15 bar, higher than the one of the reference case, where the storage pressure is set to 3.1 bar. Furthermore, in the optimum case, it can be seen the lamination process carried out by the valve installed between sections (12) and (13).

Since a peculiarity of this paper is represented by the two-phase cryogenic expander, a detailed study for this component has been carried out. The using of this device has been considered to enhance the process efficiency.

During the last decades, studies on cryogenic LNG expander have led to a development in the design and performance of this component. However, application for a two-phase expansion, such as the one described in this paper, is generally employed in large-scale plants, where vertical axis turbines are the most utilized [43]. For a small-scale case, in literature there are not many data about this component. Wang et al. [45], conducted a study to evaluate the performance of a cryogenic liquid turbine expander for liquefied nitrogen, which then works only in the liquid phase. The expander is a radial turbine consisting of an asymmetrical volute, variable stager vane nozzle ring, impeller and diffuser duct. The study considers a pressure ratio of the expander lower than 2 and a volume flow rate of 30 m^3/h. Varying the flow rate, the maximum value of isentropic efficiency of the expander (η_{is}) is 78.8 %. In addition, M. Kanoğlu [46] analyzes thermodynamic aspects of a radial inflow reaction cryogenic turbine, which works with LNG. The results show that the value of η_{is} varies from 60 to 78 %, respectively for volume flow rate through the expander of 865.8 m^3/h and 985.7 m^3/h. In the study of A. I. Prilutskii [47], a reciprocating piston expander for NG is analyzed. For mass flow rate of 3000 kg/h, the value of isentropic efficiency is 85 %. G. Habets and H. Kimmel [48] describe a method to estimate η_{is} knowing parameters like volumetric flow and rotational speed.

In this paper, to evaluate the influence of the isentropic efficiency of the expander on the system performances, a parametric analysis has been carried out. In detail, the value of η_{is} varies from 0 to 100 %, while the other parameters are set as in the optimum case, analyzed in the preceding paragraph. Then, maximum cycle pressure is 200 bar, storage pressure is 15 bar and compression chiller outlet temperature is –50 °C. In **Figure 13** and **Figure 14**, the trend of specific electric consumption and of the quality, as function of the isentropic efficiency of the expander (η_{is}), are shown. In more detail, the borderline case of η_{is} = 0%, is representative of a system configuration where the expander is replaced by a Joule-Thomson valve, that leads to an isenthalpic expansion. Therefore, the expander energy production is equal to zero. While, when η_{is} = 100%, an ideal isentropic expansion is considered. Analyzing **Figure 13** and **Figure 14**, it can be noticed that, as predictable, an increase of the isentropic efficiency leads to lower energy consumption, to a greater energy production of the expander and to lower values of the quality. These aspects are obviously tied, indeed, as already mentioned, a decrease of the quality involves a smaller system energy consumption. Furthermore, it can be pointed out that the power produced by the expander is significantly lower than the power requested by the compressors.

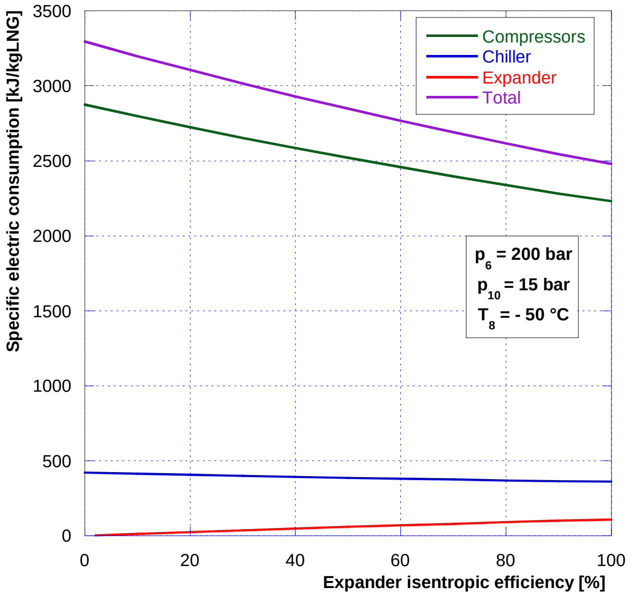

Figure 13 - Specific electric consumption/production as function of the isentropic efficiency of the expander.

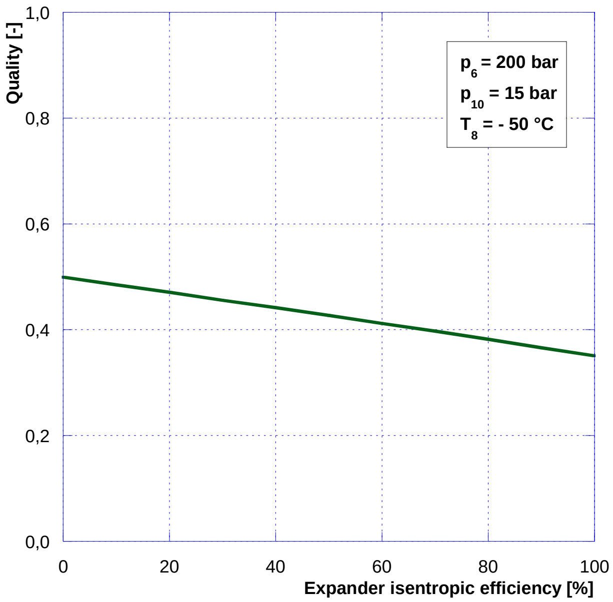

Figure 14 - Quality at the outlet of the expander as function of the isentropic efficiency of the expander.

Considering the difficulties to identify an existing machine that can perform a two-phase expansion with small mass flow, a compressor, modified to work in reverse as an expander, could represent a solution. The diagram represented in **Figure 15** (also known as Baljè diagram) is helpful for a preliminary selection of the expander [49]. In this diagram the specific speed N_S and specific diameter D_S are introduced. They are defined as follows:

$$N_S = \frac{N \cdot \sqrt{V_3}}{{H_{ad}}^{0.75}} \cdot a^{-0.75} \tag{6}$$

$$D_S = \frac{D \cdot {H_{ad}}^{0.25}}{\sqrt{V_3}} \cdot a^{0.25} \tag{7}$$

where:

- N is the rotational speed [rpm];
- D is the characteristic dimension of the expander [m] (e.g. the piston diameter in a piston expander);
- V_3 is volume flow rate at the outlet of the expander [m^3/s];
- a is a conversion factor, its value is 0.3048 [m/ft];
- H_{ad} is the adiabatic head [m]. This parameter can be expressed as:

$$H_{ad} = \frac{\Delta h_{is}}{g} \tag{8}$$

where:

- Δh_{is} is the isentropic enthalpy difference between inlet and outlet section of the expander [J/kg];
- g is the gravitational acceleration [m/s^2].

The curves in the diagram represent iso-efficiency lines for the different machine types (reciprocating expander, axial turbine, etc.).

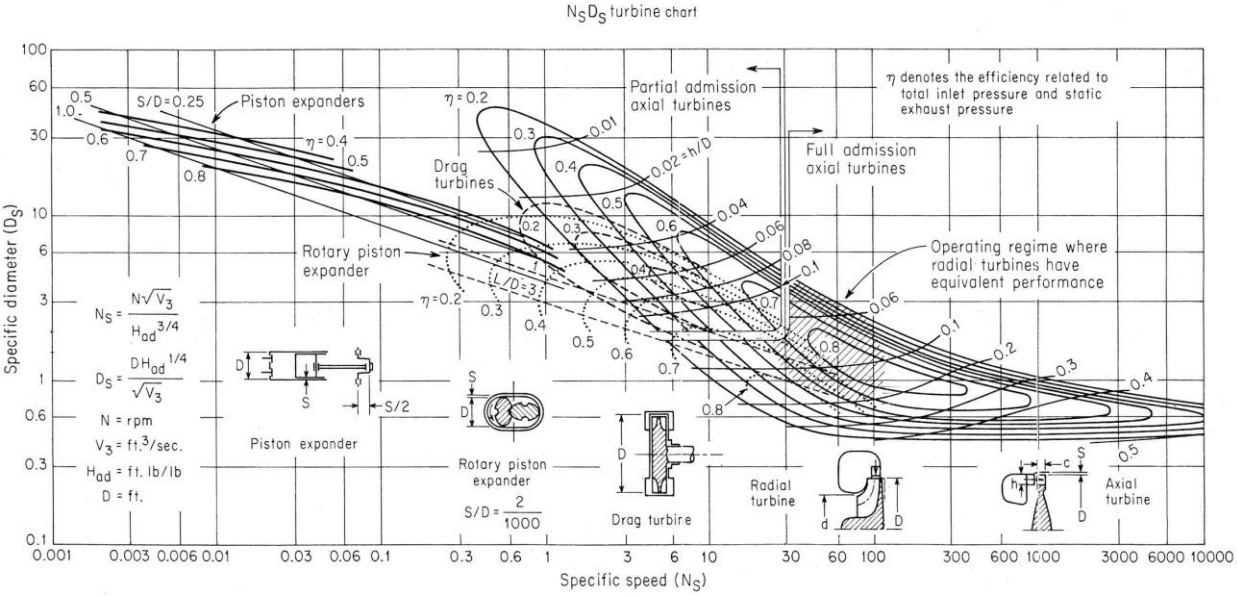

Figure 15 - N_S-D_S turbine chart [48].

The N_S-D_S diagram can be used during a preliminary design phase to choose the most suitable expander for an application or also, knowing the type of expander and the operating conditions, for determining its performances.
For example, knowing the operating conditions of the expander and either the reference length or the rotational speed, it is possible to determine N_S or D_S. At this point, the curve corresponding to the expander can be detected. Then, knowing N_S or D_S and the expander curve, the value of D_S or N_S can be find on the diagram. Finally, from this value it is possible to determine the rotational speed or the characteristic dimension of the expander.
For the system analyzed in this paper, making use of Baljè diagram, some consideration on the choice of the most suitable typology of expander for this application can be done. As example, considering a LNG mass flow rate of 0.5 kg/s, assuming the employment of a piston expander with an efficiency of 80 % and a specific speed (N_S) of 0.1, the value of rotational speed results about 400 rpm, while the value of the piston diameter is about 155 mm. On the other hand, to employ an axial expander much higher rotational speed values are required. Assuming an efficiency of the expander of 80 % and N_S = 300 (unite of measure are in line with the diagram), it results a rotational speed of about 10^6 rpm and a characteristic dimension close to 10 mm. Then, it can be noticed that the axial expanders require very low characteristic dimension and very high rotational speed that imply a complexity of the machine not reasonable for low mass flow rate such as the one of the system studied in this paper.
The problems related to a cryogenic application and a two-phase expansion will be more thoroughly assessed in future studies.

5 CONCLUSIONS

The aim of this study is the optimization of a small-scale plant for the liquefaction process of natural gas. This system is designed for *plug & play* application, in order to be used for the refueling of vehicles. Direct installation at filling stations would avoid the costs related to the liquefied natural gas transport.
The peculiarity of the system proposed in this paper is the presence of a cryogenic expander instead of a more common Joule-Thomson valve. This device allows to enhance the system efficiency, ensuring a higher liquid fraction at the end of expansion, if compared to a lamination valve. Moreover, it is possible to integrate into the process the produced shaft power. Starting from a reference case, a parametric analysis has been carried out. The key parameter considered for the optimization study is the total energy consumption of the system. Varying the maximum pressure of the cycle, the outlet temperature of the compression chiller and the storage pressure, an optimal configuration was found. The corresponding values of these parameters in the optimum case are the following: maximum pressure is 200 bar, outlet temperature of the chiller is -50 °C and storage pressure is 15 bar. The analysis points out the limited influence of the maximum pressure on the system performances. Contrarily, the outlet temperature of the chiller and the storage pressure are more influential parameters. Indeed, it can be noticed that the lower is the outlet temperature of the chiller, the lower is the quality at the outlet of the expander. The same effect on the quality can be obtained with the increase of the storage pressure. A lower quality leads to a lower vapor fraction extracted by the flash tank, which means a lower compression work, then an energy saving.

The optimum case results in a specific total electric energy consumption of 2690 kJ/kg$_{LNG}$, lower if compared to the value obtained in the reference case that is 3044 kJ/kg$_{LNG}$. Therefore, the energy saving is about 12 %. It has also been analyzed the influence of the isentropic efficiency of the expander on the system performances. As expected, the greater is the isentropic efficiency, the lower is total energy consumption. The lack of information in literature about application of two-phase cryogenic expander, such as the one analyzed in this paper, allows only a qualitative evaluation about the influence of the isentropic efficiency of the expander on the system performance. For this reason, the Baljè diagram has been introduced. This diagram is useful for a preliminary study, indeed it allows to assess what is the most suited typology of expander for the examined system.

REFERENCES

[1] ExxonMobil. 2017 Outlook for energy: A view to 2040, http://corporate.exxonmobil.com/en/energy/energy-outlook; 2017 [accessed 29.03.2017].

[2] M. Balat. Global Trends on Production and Utilization of Natural Gas. Energy Sources Part B: Economics, Planning and Policy 2009;4(4):333-346. DOI: 10.1080/15567240701621125.

[3] British Petroleum (BP). BP. Statistical review of world energy, http://www.bp.com/en/global/corporate/energy-economics/statistical-review-of-world-energy.html; 2017 [accessed 29.03.2017].

[4] W. Won, S.K. Lee, K. Choi, Y. Kwon. Current trends for the floating liquefied natural gas (FLNG) technologies. Korean Journal of Chemical Engineering 2014;31(5):732-743. DOI: 10.1007/s11814-014-0047-x.

[5] S. Kumar, H-T. Won, K-H. Choi, W. Lim, J.H. Cho, K. Tak, I. Moon. LNG: An eco-friendly cryogenic for sustainable development. Applied Energy 2011;88:4264-4273. DOI: 10.1016/j.apenergy.2011.06.035.

[6] A. Aspelund, T. Gundersen. A liquefied energy chain for transport and utilization of natural gas for power production with CO_2 capture and storage – Part 1. Applied Energy 2009;86(6):781-792. DOI: 10.1016/j.apenergy.2008.10.010.

[7] A. Aspelund, T. Gundersen. A liquefied energy chain for transport and utilization of natural gas for power production with CO_2 capture and storage – Part 2: The offshore and the onshore processes. Applied Energy 2009;86(6):793-804. DOI: 10.1016/j.apenergy.2008.10.022.

[8] A. Aspelund, S.P. Tveit, Gundersen. A liquefied energy chain for transport and utilization of natural gas for power production with CO_2 capture and storage – Part 3: The combined carrier and onshore storages. Applied Energy 2009;86(6):805-814. DOI: 10.1016/j.apenergy.2008.10.023.

[9] A. Aspelund, T. Gundersen. A liquefied energy chain for transport and utilization of natural gas for power production with CO_2 capture and storage – Part 4: Sensitivity analysis of transport pressures and benchmarking with conventional technology for gas transport. Applied Energy 2009;86(6):815-825. DOI: 10.1016/j.apenergy.2008.10.021.

[10] H. Cho, Y. Yeo, J. Kim. Optimal design of natural gas liquefaction processes. Korean Chem Eng Res 2013;51(1):25-34. DOI: 10.9713/kcer.2013.51.1.25.

[11] MJ Kim, GB Yi, J. Liu. Determination of mixing ratio of mixed refrigerants and performance analysis of natural gas liquefaction processes. Korean Journal of Chemical Engineering 2013;51:677-684. DOI: 10.9713/kcer.2013.51.6.677.

[12] N.B.N. Khan, A. Barifcani, M. Tade, V. Pareek. A case study: Application of energy and exergy analysis for enhancing the process efficiency of a three stage propane pre-cooling cycle of the cascade LNG process. Journal of Natural Gas Science and Engineering 2016;29:125-133. DOI: 10.1016/j.jngse.2015.12.034.

[13] B. Ghorbani, M.H. Hamedi, M. Amidpour, M. Mehrpooya. Cascade refrigeration systems in integrated cryogenic natural gas process (natural gas liquids (NGL), liquefied natural gas (LNG) and nitrogen rejection unit (NRU)). Energy 2016;15:88-106. DOI: 10.1016/j.energy.2016.09.005.

[14] A. Kilicarslan, M. Hosoz. Energy and irreversibility analysis of a cascade refrigeration system for various refrigerant couples. Energy Conversion and Management 2010;51(12):2947-2954. DOI: 10.1016/j.enconman.2010.06.037.

[15] M.F.M. Fahmy, H.I. Nabih, M. El-Nigeily. Enhancement of the efficiency of the Open Cycle Phillips Optimized Cascade LNG process. Energy Conversion and Management 2016;12:308-318. DOI: 10.1016/j.enconman.2016.01.022.

[16] S. Lee. Multi-parameter optimization of cold energy recovery in cascade Rankine cycle for LNG regasification using genetic algorithm. Energy 2017;118:776-782. DOI: 10.1016/j.energy.2016.10.118.

[17] Y. He, R. Li, G. Chen, Y. Wang. A potential auto-cascade absorption refrigeration system for pre-cooling of LNG liquefaction. Journal of Natural Gas Science and Engineering 2015;24:425-430. DOI: 10.1016/j.jngse.2015.03.035.

[18] T. He, Y. Ju. Dynamic simulation of mixed refrigerant process for small-scale LNG plant in skid mount packages. Energy 2016;97:350-358. DOI: 10.1016/j.energy.2016.01.001.

[19] L. Cao, J. Liu, X. Xu. Robustness analysis of the mixed refrigerant composition employed in the single mixed refrigerant (SMR) liquefied natural gas (LNG) process. Applied Thermal Engineering 2016;93:1155-1163. DOI: 10.1016/j.applthermaleng.2015.10.072.

[20] M. Wang, R. Khalilpour, A. Abbas. Thermodynamic and economic optimization of LNG mixed refrigerant processes. Energy Conversion and Management 2014;88:947-961. DOI: 10.1016/j.enconman.2014.09.007.

[21] M. S. Khan, S. Lee, G.P. Rangaiah, M. Lee. Knowledge based decision making method for the selection of mixed refrigerant systems for energy efficient LNG processes. Applied Energy 2013;111:1018-1031. DOI: 10.1016/j.apenergy.2013.06.010.

[22] J-H. Hwang, M-I. Roh, K-Y. Lee. Determination of the optimal operating conditions of the dual mixed refrigerant cycle for the LNG FPSO topside liquefaction process. Computers & Chemical Engineering 2013;49:25-36. DOI: 10.1016/j.compchemeng.2012.09.008.

[23] A. Mortazavi, C. Somers, Y. Hwang, R. Radermacher, P. Rodgers, S. Al-Hashimi. Performance enhancement of propane pre-cooled mixed refrigerant LNG plant. Applied Energy 2012;93:123-131. DOI: 10.1016/j.apenergy.2011.05.009.

[24] H-M. Chang. A thermodynamic review of cryogenic refrigeration cycles for liquefaction of natural gas. Cryogenics 2015;72:127-147. DOI: 10.1016/j.cryogenics.2015.10.003.

[25] B. Austbø, T. Gundersen. Optimization of a Single Expander LNG Process. Energy Procedia 2015;64:63-72. DOI: 10.1016/j.egypro.2015.01.009.

[26] P. Moein, M. Sarmad, M. Khakpour, H. Delaram. Methane addition effect on a dual nitrogen expander refrigeration cycle for LNG production. Journal of Natural Gas Science and Engineering 2016;33:1-7. DOI: 10.1016/j.jngse.2016.04.061.

[27] W. Lim, I. Lee, K. Lee, B. Lyu, J. Kim, I. Moon. Design and analysis of multi-stage expander processes for liquefying natural gas. Korean Journal of Chemical Engineering 2014;31(9):1522-1531. DOI: 10.1007/s11814-014-0098-z.

[28] T. He, Y. Ju. Optimal synthesis of expansion liquefaction cycle for distributed-scale LNG (liquefied natural gas) plant. Energy 2015;88:268-280. DOI: 10.1016/j.energy.2015.05.046.

[29] M. S. Khan, S. Lee, M. Getu, M. Lee. Knowledge inspired investigation of selected parameters on energy consumption in nitrogen single and dual expander processes of natural gas liquefaction. Journal of Natural Gas Science and Engineering 2015;23:324-337. DOI: 10.1016/j.jngse.2015.02.008.

[30] Y. Li, X. Wang, Y. Ding. An optimal design methodology for large-scale gas liquefaction. Applied Energy 2012;99:484-490. DOI: 10.1016/j.apenergy.2012.04.040.

[31] C.W. Remeljej, A.F.A. Hoadley. An exergy analysis of small-scale liquefied natural gas (LNG) liquefaction processes. Energy 2004;31(12):2005-2019. DOI: 10.1016/j.energy.2005.09.005.

[32] W. Lim, K. Choi, I. Moon. Current Status and Perspectives of Liquefied Natural Gas (LNG) Plant Design. Industrial & Engineering Chemistry Research 2013;52(9):3065-3088. DOI: 10.1021/ie302877g.

[33] I. Maynitskiy. The Evolution of Small-Scale LNG Market. in Small-Scale LNG Forum, Istanbul, 2012.

[34] Visiongain. Small scale liquefied natural gas (LNG) market 2015-2025, https://www.visiongain.com/Report/1383/Small-Scale-Liquefied-Natural-Gas-(LNG)-Market-2015-2025; 2015 [accessed 05.01.2017].

[35] X. Xu, J. Liu, C. Jiang, L.Cao. The correlation between mixed refrigerant composition and ambient conditions in the PRICO LNG process. Applied Energy 2013;102:1127-1136. DOI: 10.1016/j.apenergy.2012.06.031.

[36] T. Gao, W. Lin, A. Gu, M. Gu. Coalbed methane liquefaction adopting a nitrogen expansion process with propane pre-cooling. Applied Energy 2010;87(7):2142-2147. DOI: 10.1016/j.apenergy.2009.12.010.

[37] J. Kim, Y. Seo, D. Chang. Economic evaluation of a new small-scale LNG supply chain using liquid nitrogen for natural-gas liquefaction. Applied Energy 2016;182:154-163. DOI: 10.1016/j.apenergy.2016.08.130.

[38] Z. Yuan, M. Cui, Y. Xie, C. Li. Design analysis of a small-scale natural gas liquefaction process adopting single nitrogen expansion with carbon dioxide pre-cooling. Applied Thermal Engineering 2014;64(1-2):139-146. DOI: 10.1016/j.applthermaleng.2013.12.011.

[39] T.B. He, Y.L. Ju. A novel process for small-scale pipeline natural gas liquefaction. Applied Energy 2014;115:17-24. DOI: 10.1016/j.apenergy.2013.11.016.

[40] R. Jokinen, F. Pettersson, H. Saxén. An MILP model for optimization of a small-scale LNG supply chain along a coastline. Applied Energy 2015;138:423-431. DOI: 10.1016/j.apenergy.2014.10.039.

[41] M. A. Ancona, M. Bianchi, L. Branchini, A. De Pascale, F. Melino. A Novel Small Scale Liquefied Natural Gas Production Process at Filling Stations: Thermodynamic Analysis and Parametric Investigation. in ASME Turbo Expo 2016: Power for Land, Sea and Air, Seoul, 2016. DOI: 10.1115/GT2016-56463.

[42] M. A. Ancona, M. Bianchi, L. Branchini, A. De Pascale, F. Melino. Performance Increase of a Small-scale Liquefied Natural Gas Production Process by Means of Turbo-Expander. International Conference on Applied Energy ICAE 2016 Oct 8-11, Beijing, China.

[43] V. P. Patel, H. E. Kimmel. Fifteen Years of Field Experience in LNG Expander Technology. in Proceedings of the First Middle East Turbomachinery Symposium, Doha, 2011.

[44] Asimptote. FluidProp, http://www.asimptote.nl/software/fluidprop; [accessed 29.03.2017].

[45] K. Wang, J. Sun, P. Song. Experimental study of cryogenic liquid turbine expander with closed-loop liquefied nitrogen system. Cryogenics 2015;67:4-14. DOI: 10.1016/j.cryogenics.2015.01.004.

[46] M. Kanoğlu. Cryogenic turbine efficiencies. Exergy, An International Journal 2001;1:202-208.

DOI: 10.1016/S1164-0235(01)00026-7.
[47] A. I. Prilutskii. Use of piston expanders in plants utilizing energy of compressed natural gas. Chemical and Petroleum Engineering 2008;44(3):149-156. DOI: 10.1007/s10556-008-9027-5.
[48] G. Habets, H. Kimmel. Economics of cryogenic turbine expanders. The International Journal of Hydrocarbon Engineering, 1998.
[49] E. Kenneth, P.E. Nichols. Barber-Nichols. How to select turbomachinery for your application. Barber-Nichols Inc. http://www.barber-nichols.com.

APPENDIX A

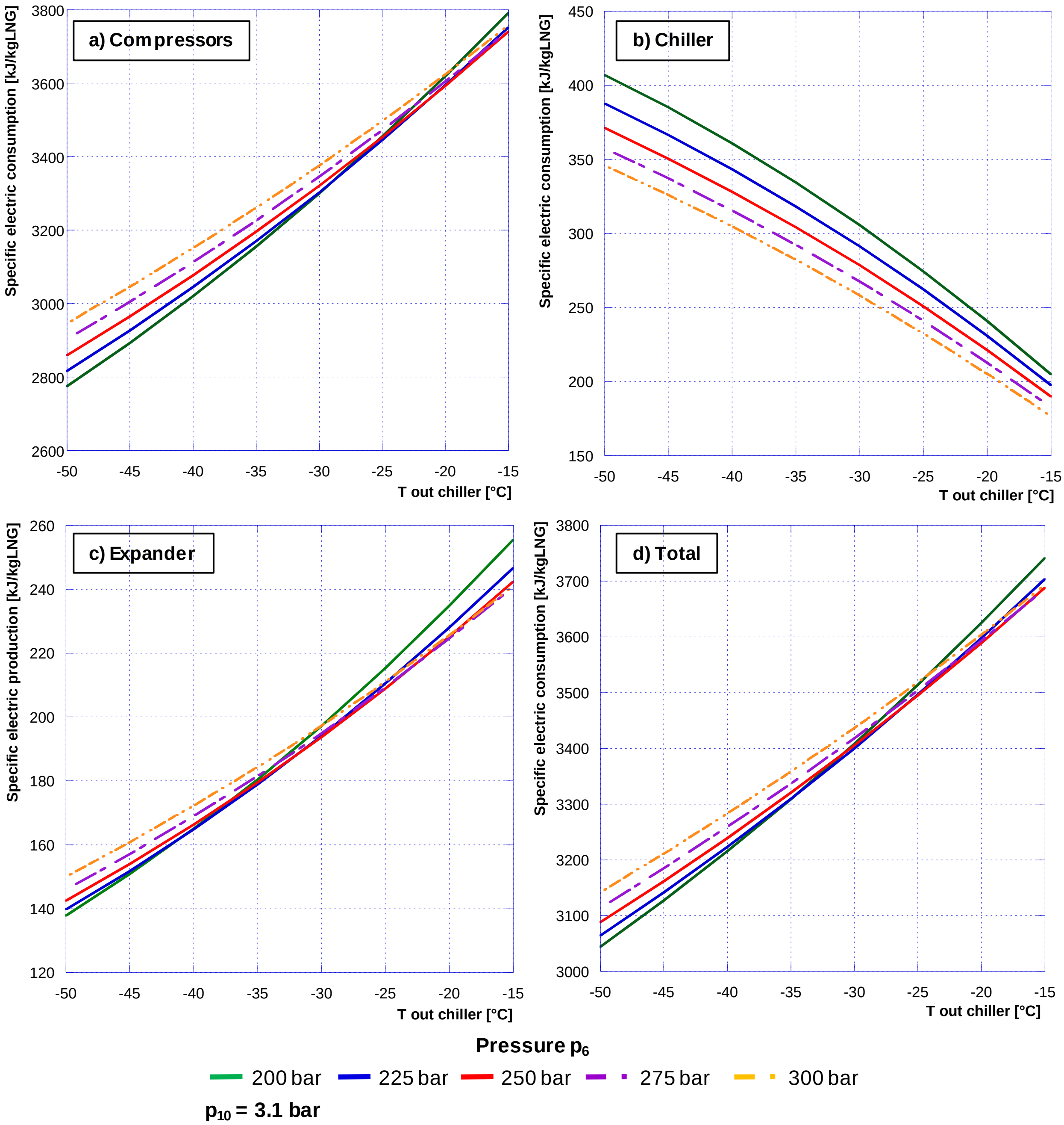

Figure A1 - Specific electric energy consumption/production of the components as function of the outlet temperature of the chiller (T_8) for several values of maximum pressure p_6, with a set value of storage pressure p_{10} = 3.1 bar.

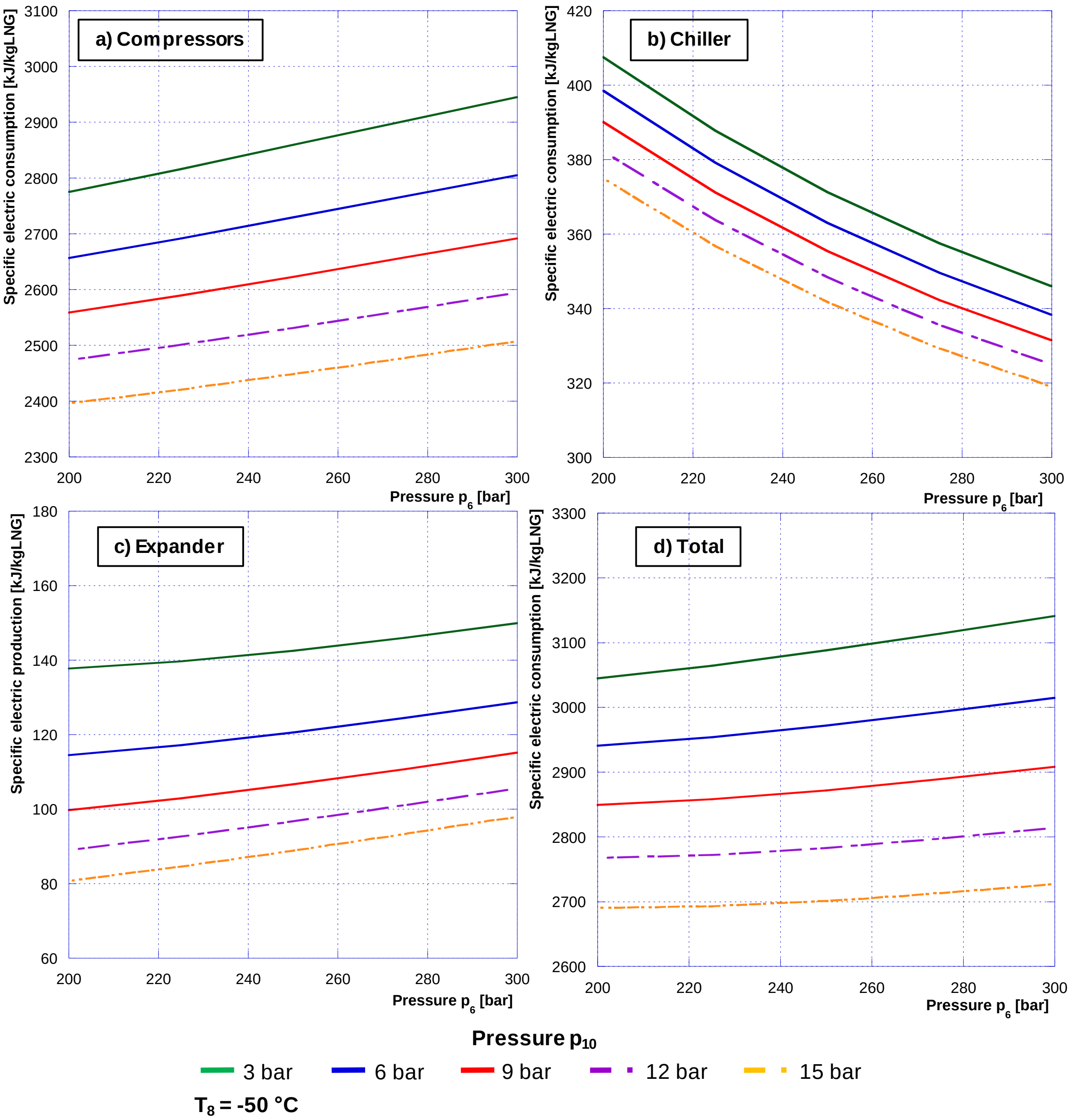

555

556 **Figure A2** - Specific electric energy consumption/production of the components as function of maximum pressure p_6, for
557 several values of storage pressure p_{10} and a set value of T_8 = -50 °C.

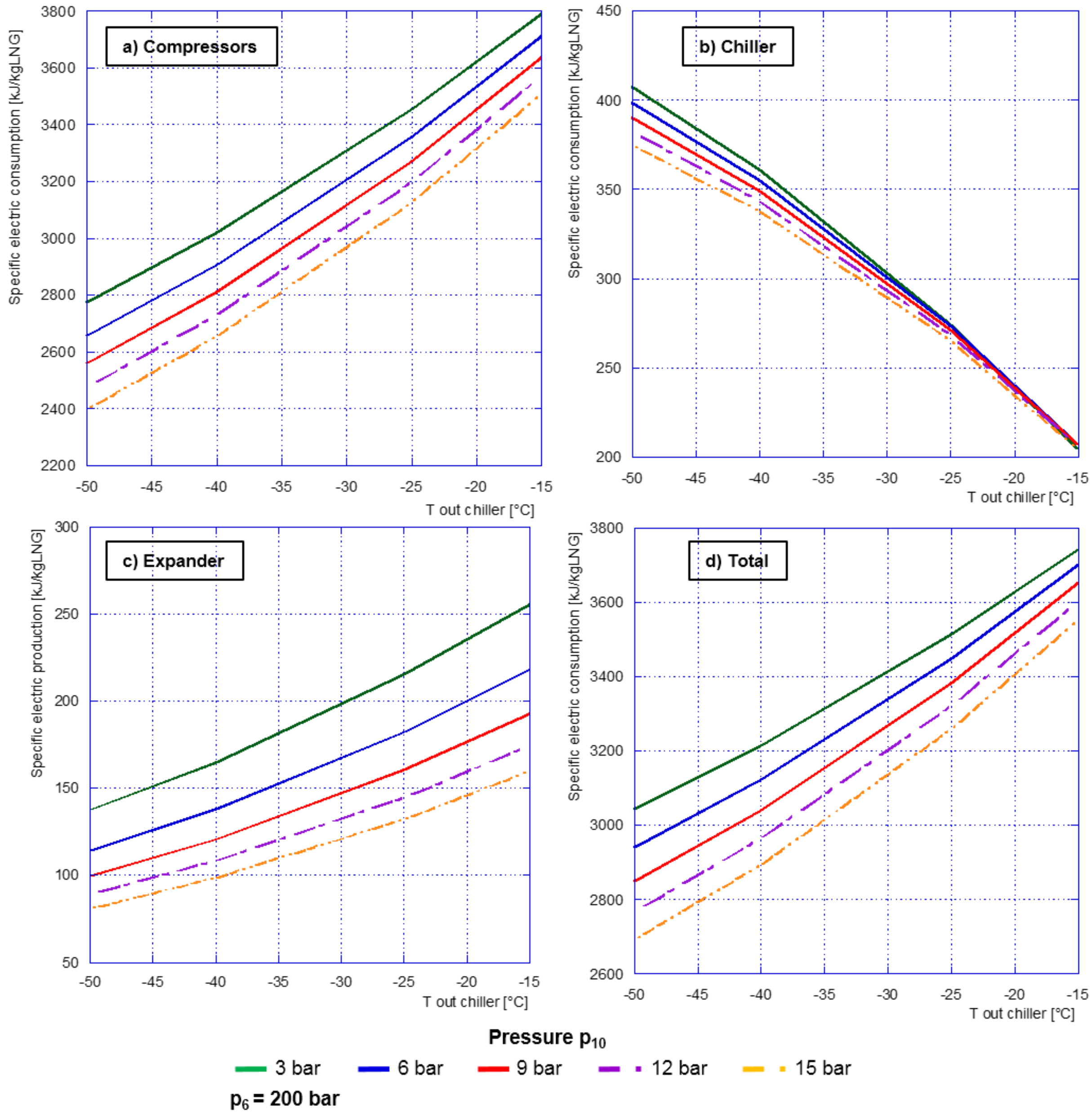

558

559 **Figure A3 -** Specific electric energy consumption/production of the components as function of outlet temperature of the chiller
560 T_8, for several values of storage pressure p_{10} and a set value of maximum pressure p_6 = 200 bar.